Journal of Nepal Hydrogeological Association (JNHA), Vol (2), 45-65 (2025)
ISSN: 3059-9725 (Online)
https://doi.org/10.3126/jnha.v2i1.85379

RESEARCH ARTICLE

Deformation and support analysis of headrace tunnels in three tectonic zones of Nepal: An empirical and numerical approach

Ijan Shrestha, Balkrishna Jha, Aashika Koju, Aanand Kumar Mishra, *Nirmal Kafle

Department of Civil Engineering, Khwopa College of Engineering,
Tribhuvan University, Nepal
**Corresponding author: nirmalkafle1917@gmail.com*

***(Submission Date**: 26 May, 2025; **Accepted Date:** 9 July, 2025)*

ABSTRACT

Tunneling in the Himalayan region presents significant engineering challenges due to complex geological formations, high seismicity, and variable rock mass conditions. This study focuses on the comparative analysis of headrace tunnels (HRTs) in three distinct geological regions of Nepal: the Siwaliks, the Lesser Himalayas, and the Higher Himalayas. The primary objective of this study is to evaluate stresses due to tunnel excavation, required support systems, and displacement in these distinct geological settings. The methodology used in this study includes empirical, and numerical approaches to assess tunnel performance in the selected regions. Finite Element Analysis (FEA) was performed to assess tunnel stability, in-situ stresses, and effectiveness of support systems. The findings show significant variations in stress generated, displacement, and required support systems across the three geological regions. The comparative analysis indicates that tunnels in weaker rock formations, like those in the Siwaliks, require substantial support systems, whereas tunnels in the Higher Himalayas experience higher in-situ stresses. This study highlights the behavior of rock masses, the consequent stresses and displacements and the required support systems in the three geological settings when constructing tunnels of the same shape and size.

Keywords: ***Displacement, FEA, Himalayas, Rock mass classification, Support systems***

INTRODUCTION

Background and Significance

The Himalayan range was formed as a consequence of the ongoing convergence and collision between the Indian and Eurasian plates, a process that began around 40 to 50 million years ago and continues today, thereby making the region seismically active (Yin and Harrison, 2000). The dynamic plate movement, combined with complex topography, contributes to frequent geological hazards such as earthquakes, landslides, and slope failures. The Nepal Himalayas is divided into several tectonic zones separated by major thrust faults, significantly influencing underground construction challenges (Paudyal and Panthi, 2010).

Complex topography and geological diversity of Nepal pose substantial challenges to underground excavation works (Panthi, 2004). Major problems encountered during tunneling in fault zones are excessive spalling, displacements, creep, and excessive water inflows. Fragile geological conditions and tectonic stresses have contributed

to the rock mass of Nepal Himalayas to be highly deformed, weathered, folded and faulted (Upreti, 1999). Proper support system must be installed during underground construction. Under estimation of support system leads to failure of the structure while over estimation leads to unnecessary increasing cost of the project.

A comparative analysis is carried out in this study for headrace tunnels (HRTs) located in three distinct geological regions of Nepal: The Siwaliks, the Lesser Himalayas and the Higher Himalayas. HRTs from the three proposed hydropower projects were analyzed and designed for the study. For each tunnel, the optimum diameter was deter- mined based on tunnel hydraulics and estimated construction costs. The average of the three optimized diameters, which was 4.4 meters, was then taken as the representative value for further evaluation. Each tunnel, with an inverted D-shaped profile, serves as a case for examining how geological variations influence tunnel behavior.

Research Gap

Although tunnel construction in the Himalayas is increasing, few studies have conducted a systematic comparison of tunnel deformation and support systems across different geological zones using both empirical and numerical methods (Abbas et al., 2024; Azad et al., 2023; Thapaliya et al., 2025). Most existing works are project-specific and lack an integrated framework that accounts for variations in rock mass behavior, stress redistribution, and support optimization.

This study addresses this gap by applying consistent empirical and finite element modeling approaches to analyze tunnel behavior in the Siwaliks, Lesser Himalayas, and Higher Himalayas. It aims to provide comparative insights that support effective and geology-specific tunnel design strategies.

Research Questions

The central research questions are:

1. How do rock mass properties and overburden depth affect tunnel-induced stresses and displacements across different Himalayan tectonic zones?
2. What are the support system variations required for tunnels in the Siwaliks, Lesser Himalayas, and Higher Himalayas?
3. How effective is the integration of empirical classification systems with numerical models for predicting tunnel deformation and optimizing support design?

By addressing these questions, the study enhances the understanding of tectonic zone-specific tunnel behavior and offers practical guidance for safe and cost-effective tunnel engineering in the Himalayan region.

STUDY AREA

The study focuses on three headrace tunnels (HRTs): Super Lower Bagmati Hydropower Project (SLBHP) in the Siwaliks, Ranma Khola Hydropower Project (RKHP) in the Lesser Himalayas, and Humla Karnali Hydropower Project (HKHP) in the Higher Himalayas as shown in Fig 1.

The SLBHP lies in the Siwaliks region, which is a young sedimentary zone comprising mudstone and sand- stone. RKHP is situated in the Lesser Himalayas, where the rock mass mainly consists of moderately weathered quartzite and phyllite. HKHP is located in the Higher Himalayas characterized by high-grade metamorphic rocks like augen gneiss.

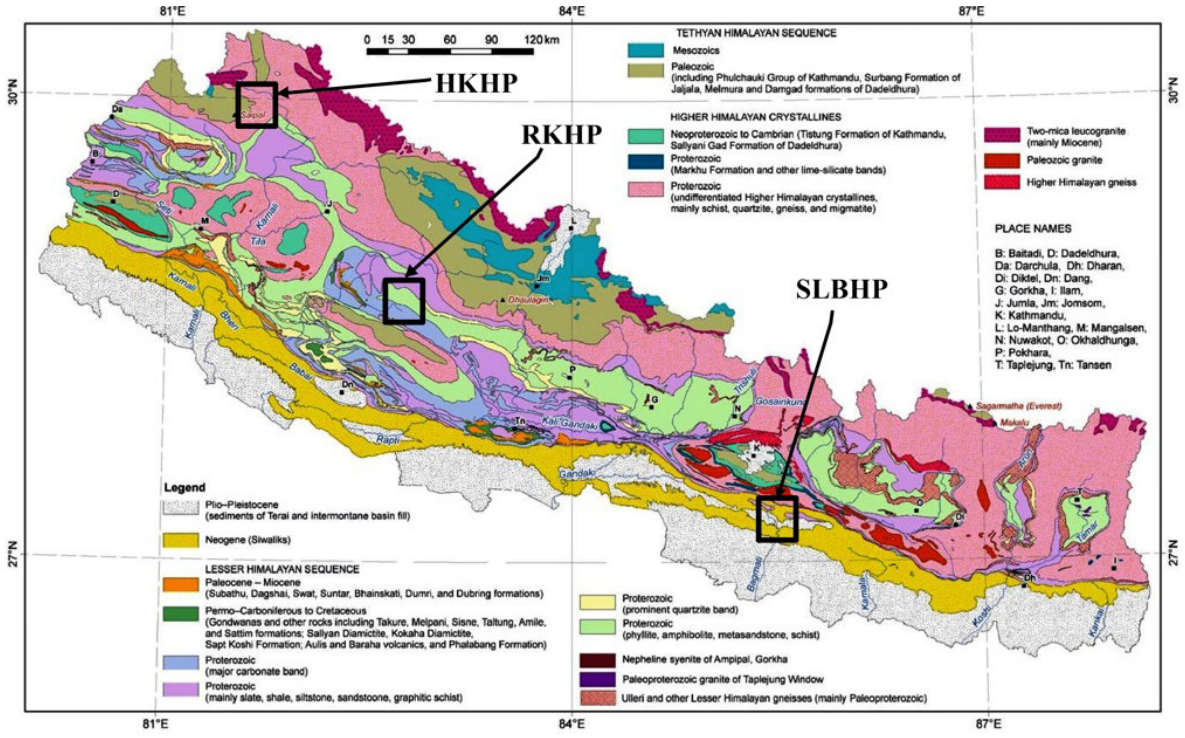

Fig. 1: Geological map of Nepal showing the study sreas *(Dhital, 2015)*

MATERIALS AND METHODS

Empirical methods and FEA were used to conduct the comparative analysis of HRTs in three distinct geological regions of Nepal.

SITE SELECTION AND DATA COLLECTION

The site selection for this study was based on three representative hydropower tunnel projects situated across Nepal's primary geological zones: the Siwaliks, the Lesser Himalayas, and the Higher Himalayas. The selected projects are either proposed or under construction and offer a diverse range of geological conditions suitable for comparative analysis.

Data collection was conducted exclusively using secondary sources, including design documents and geological investigation reports from consulting firms. These documents provided details on lithology, rock mass classification parameters (RMR, Q-values), overburden depth, deformation modulus, and proposed support systems. Geological Strength Index (GSI) values, intact rock properties (σ_{ci}, m_i), and stress ratio parameters were derived using empirical correlations from established literature. These secondary data were cross-referenced and validated using geological maps provided by the (Dhital, 2015) Though no direct field investigation or instrumentation data was collected, the reliability of the secondary data was ensured by selecting well-documented projects and comparing results across multiple literature sources.

ROCK MASS CLASSIFICATION

The rock mass at the tunnel sites was classified using the Rock Mass Rating (RMR) system, as proposed by Bieniawski (1989), which remains one of the most widely adopted empirical classification systems in underground excavation design. Although the Q-system was not directly applied for

classification in this study, it was utilized indirectly through empirical correlations with RMR to derive essential input parameters for numerical modeling. Among the various empirical relationships proposed to interrelate RMR and Q, the correlation developed by Rutledge and Preston, as cited by Marinos et al. (2007) was identified as having the highest relevance and applicability for Himalayan rock masses. This relationship is given by:

$$RMR = 5.9lnQ + 43 \quad \text{.....(1)}$$

This equation was used to estimate Q-values from RMR values, facilitating the derivation of additional rock mass properties required for deformation modulus estimation and input to the generalized Hoek–Brown failure criterion.

ESTIMATION OF IN-SITU DEFORMATION MODULUS

The in-situ deformation modulus (E_m) of rock mass is an essential parameter for numerical modeling and stability analysis. It was estimated empirically using correlations between RMR and Q values as follows:

$$E_m = 2 \times RMR - 100 \quad \text{.....(2)}$$

For moderately poor rock quality (RMR between 30 and 55), the expression developed by (Serafim and Pereira, 1983) was applied:

$$E_m = 10^{\frac{RMR-10}{40}} \quad \text{.....(3)}$$

For rock masses where Q values were greater than 1, the empirical formula from (Grimstad and Barton, 1993) was used:

$$E_m = 25log_{10}Q \quad \text{.....(4)}$$

Table 1: Average in-situ deformation modulus obtained along the HRTs

	Chainage	Rock Type	RMR	Q	Overburden (m)	E_m (GPa)
Siwaliks	0+000 - 1+600	Sandstone	45	1.12	416.160	4.353
	1+600 - 3+700	Sandstone	40	0.64	496.957	2.812
	3+700 - 5+600	Mudstone	31	0.21	479.730	1.581
	5+600 - 6+888	Sandstone	32	0.26	165.499	1.774
	Chainage	Rock Type	RMR	Q	Overburden (m)	E_m (GPa)

Lesser Himalaya	0+000 - 0+550	Quartzite	62	2.23	521	16.34
	0+550 - 1+500	Quartzite	66	2.91	749	21.79
	1+500 - 3+250	Sandstone	63	2.38	770	17.70
	3+250 - 4+000	Sandstone	64	2.54	702	19.07
	4+000 - 4+900	Sandstone	56	1.49	495	8.17
	4+900 - 6+000	Sandstone	61	2.08	736	14.98
	6+000 - 7+690	Sandstone	54	1.31	593	7.74

	Chainage	Rock Type	RMR	Q	Overburden (m)	E_m (GPa)
Higher Himalaya	0+000 - 1+150	Augen Gneiss	74	4.63	515	31.32
	1+150 - 3+300	Augen Gneiss	63	2.38	306	17.70
	3+300 - 4+300	Augen Gneiss	68	3.32	305	24.51
	4+300 - 6+880	Augen Gneiss	65	2.91	435	21.79

Determination of Parameters for Generalized Hoek–Brown Failure Criterion

In order to simulate the behavior of the rockmass, the generalized Hoek–Brown failure criterion was adopted to define the strength envelope in numerical modeling. The generalized Hoek–Brown criterion is expressed as follows (Hoek and Brown, 2018):

$$\sigma_1 = \sigma_3 + \sigma_{ci}\left(m_b \frac{\sigma_3}{\sigma_{ci}} + s\right)^a \quad \text{.....(5)}$$

where:

- σ_1 = major principal stress at failure
- σ_3 = minor principal stress

The following empirical relationships were used to derive the Hoek–Brown parameters:

$$m_b = m_i e^{\frac{GSI-100}{28}} \quad \text{.....(7)}$$

$$s = e^{\frac{GSI-100}{9}} \quad \text{.....(8)}$$

$$a = \frac{1}{2} + \frac{1}{6}\left(e^{-\frac{GSI}{15}} - e^{-\frac{20}{3}}\right) \quad \text{.....(9)}$$

Where m_i is the intact rock constant, determined from laboratory uniaxial compression tests or adopted from standard literature values for the encountered rock types.

The horizontal-to-vertical stress ratio (k) was computed based on the empirical equation proposed by (Sheorey, 1994):

• σ_{ci} = uniaxial compressive strength of intact rock
• m_b = reduced material constant for the rockmass
• s and a = constants that account for rock mass quality.

The parameters m_b, s and a were calculated based on the Geological Strength Index (GSI) and the intact rock constant m_i. Relation between Geological Strength Index (GSI) and RMR as per (Hoek and Diederichs, 2006) was used to calculate GSI which is given as:

$$GSI = RMR - 5 \quad \text{..... (6)}$$

$$k = 0.25 + 7 \times E_m (0.001 + \frac{1}{z}) \quad \text{..... (10)}$$

• E_m = in-situ deformation modulus (GPa),
• z = overburden (m)

The Disturbance Factor (D) is a parameter that accounts for the extent of disturbance or relaxation in the rockmass due to excavation and blasting activities.

In addition to strength parameters, Poisson's ratio of the rockmass was calculated using the relation suggested by (Aydan, 2019), that can be stated as:

$$\upsilon_{rm} = 0.5 - 0.2 \times \frac{RMR}{RMR + 0.2 \times (100 - RMR)} \quad \text{.....(11)}$$

Table 2: Parameters used for Generalized Hoek–Brown failure criterion along the HRTs

	Chainage	k	D	GSI	υ_{rm}	m_i	m_b	s	a	σ_{ci} (MPa)
Siwaliks	0+000 - 1+600	0.35	0.7	40	0.35	8	0.31	0.0002	0.51	114.4
	1+600 - 3+700	0.31	0.7	35	0.35	19	0.48	0.0001	0.52	114.4
	3+700 - 5+600	0.28	0.7	25	0.38	9	0.07	0.0007	0.53	63.0
	5+600 - 6+888	0.34	0.7	27	0.37	9	0.11	0.0005	0.53	114.4
	Chainage	k	D	GSI	υ_{rm}	m_i	m_b	s	a	σ_{ci} (MPa)
Lesser Himalaya	0+000 - 0+550	0.58	0.6	57	0.32	24	3.65	0.0043	0.5	214.9
	0+550 - 1+500	0.61	0.6	61	0.32	24	4.35	0.0071	0.5	214.9
	1+500 - 3+250	0.53	0.6	58	0.32	19	3.02	0.0049	0.5	150.0
	3+250 - 4+000	0.57	0.6	59	0.32	19	2.21	0.0018	0.51	150.0
	4+000 - 4+900	0.42	0.6	51	0.33	19	2.07	0.0018	0.51	150.0
	4+900 - 6+000	0.5	0.6	66	0.32	19	2.76	0.0038	0.50	150.0
	6+000 - 7+690	0.4	0.6	49	0.33	19	3.07	0.0035	0.51	150.0

	Chainage	k	D	GSI	υ_{rm}	m_i	m_b	s	a	σ_{ci} (MPa)
Higher Himalaya	0+000 - 1+150	0.59	0.5	68	0.32	25	6.10	0.0171	0.51	233.5
	1+150 - 3+300	0.90	0.5	58	0.33	25	4.82	0.0560	0.5	233.5
	3+300 - 4+300	0.78	0.5	63	0.32	25	5.30	0.0106	0.5	233.5
	4+300 - 6+880	0.69	0.5	61	0.32	25	4.86	0.0081	0.5	233.5

Finite Element Analysis

The HRTs were modeled numerically to simulate the stress distribution and deformation around tunnel excavations. The input parameters for the simulations such as rock mass properties, in-situ stress conditions, boundary conditions, and support configurations were derived from empirical classification systems (RMR and Q-system) and field investigations. The modeling process involved:

- Simulating tunnel behavior before and after support installation
- Analyzing principal stresses and displacement patterns
- Optimizing Support Systems as suggested by RMR

Tunnel excavation was simulated in 15 stages at random intervals to reflect real-world variability in geological and operational conditions. A graded mesh of 3-noded triangular elements (gradation factor 0.1) was used to increase density near tunnel boundaries which is critical for stress and deformation. This approach improved accuracy in capturing stress redistribution while optimizing computation. The mesh generated contained 150 nodes, which provided a compromise between model detail and processing time.

Tunnel Support Design and Optimization

Tunnel support design was initially done as suggested by RMR, providing baseline configurations for fiber-reinforced shotcrete (FRS), rock bolts, and steel sets. The properties of the FRS used in the modeling was based on the studies of (Shah and Rangan, 1971). The principles used for rock bolt design were guided by the work of (Li, 2017). The supports were then optimized to ensure effective load transfer and to maintain a factor of safety of 1.5.

DATA ANALYSIS

The data obtained from field investigations was used for numerical modeling and support system design. The in-situ deformation modulus of the rock mass was calculated for different chainages along the HRT alignment based on the RMR and Q values. The calculated average values of deformation modulus at various chainages are presented in Table 1. Likewise, the parameters used for the Hoek–Brown Failure Criterion is presented in Table 2 .

Table 3 Empirical support systems of each tectonic zone along the HRTs

	Chainage	Rock Type	RMR	Q	Support System According to RMR	Support System According to Q
Siwaliks	0+000 - 1+600	Sandstone	45	1.12	Systematic bolts 4 m long, spaced 1.5 m to 2 m in crown and wall with wire mesh in crown, 50 mm to 100 mm shotcrete in crown and 30 mm in walls.	Rockbolts of length 3.5 m long, spaced 2 m, 100 mm thick shotcrete
	1+600 - 3+700	Sandstone	40	0.64	Systematic bolts 4 m to 5m long, spaced 1 m to 1.5 m in crown and wall with wire mesh, 100 mm to 150 mm shotcrete in crown and 100 mm in walls, light to medium ribs spaces 1.5 m where required.	Rockbolts of length 3.5 m long, spaced 2 m, 110 mm thick shotcrete
	3+700 - 5+600	Mudstone	31	0.21	Systematic bolts 4 m to 5m long, spaced 1 m to 1.5 m in crown and wall with wire mesh, 100 mm to 150 mm shotcrete in crown and 100 mm in walls, light to medium ribs spaces 1.5 m where required.	Rockbolts of length 3.5 m long, spaced 2 m, 110 mm thick shotcrete
	5+600 - 6+888	Sandstone	32	0.26	Systematic bolts 4 m to 5m long, spaced 1 m to 1.5 m in crown and wall with wire mesh, 100 mm to 150 mm shotcrete in crown and 100 mm in walls, light to medium ribs spaces 1.5 m where required.	Rockbolts of length 3.5 m long, spaced 2 m, 110 mm thick shotcrete

	Chainage	Rock Type	RMR	Q	Support System According to RMR	Support System According to Q
Lesser Himalaya	0+000 - 0+550	Quartzite	62	2.23	Locally bolts in crown 3 m long, spaced 2.5 m with occasional wire mesh, 50 mm shotcrete in crown where required.	Rockbolts of length 3 m long, spaced 2 m, 80 mm thick shotcrete
	0+550 - 1+500	Quartzite	66	2.91	Locally bolts in crown 3 m long, spaced 2.5 m with occasional wire mesh, 50 mm shotcrete in crown where required.	Rockbolts of length 3 m long, spaced 2 m, 60 mm thick shotcrete
	1+500 - 3+250	Sandstone	63	2.38	Locally bolts in crown 3 m long, spaced 2.5 m with occasional wire mesh, 50 mm shotcrete in crown where required.	Rockbolts of length 3 m long, spaced 2 m, 65 mm thick shotcrete
	3+250 - 4+000	Sandstone	64	2.54	Locally bolts in crown 3 m long, spaced 2.5 m with occasional wire mesh, 50 mm shotcrete in crown where required.	Rockbolts of length 3 m long, spaced 2 m, 65 mm thick shotcrete
	4+000 - 4+900	Sandstone	56	1.49	Systematic bolts 4 m long, spaced 1.5 m to 2 m in crown and wall with wire mesh in crown, 50 mm to 100 mm shotcrete in crown and 30 mm in walls.	Rockbolts of length 3 m long, spaced 2 m, 85 mm thick shotcrete
	4+900 - 6+000	Sandstone	61	2.08	Locally bolts in crown 3 m long, spaced 2.5 m with occasional wire mesh, 50 mm shotcrete in crown where required.	Rockbolts of length 3 m long, spaced 2 m, 80 mm thick shotcrete
	6+000 - 7+690	Sandstone	54	1.31	Systematic bolts 4 m long, spaced 1.5 m to 2 m in crown and wall with wire mesh in crown, 50 mm to 100 mm shotcrete in crown and 30 mm in walls.	Rockbolts of length 3 m long, spaced 2 m, 85 mm thick shotcrete

	Chainage	Rock Type	RMR	Q	Support System According to RMR	Support System According to Q
Higher Himalaya	0+000 - 1+150	Augen Gneiss	74	4.63	Locally bolts in crown 3 m long, spaced 2.5 m with occasional wire mesh, 50 mm shotcrete in crown where required.	Rockbolts of length 2.6 m long, spaced 2.2 m, 60 mm thick shotcrete
	1+150 - 3+300	Augen Gneiss	63	2.38	Locally bolts in crown 3 m long, spaced 2.5 m with occasional wire mesh, 50 mm shotcrete in crown where required.	Rockbolts of length 2.6 m long, spaced 2.2 m, 65 mm thick shotcrete
	3+300 - 4+300	Augen Gneiss	68	3.32	Locally bolts in crown 3 m long, spaced 2.5 m with occasional wire mesh, 50 mm shotcrete in crown where required.	Rockbolts of length 2.6 m long, spaced 2.2 m, 60 mm thick shotcrete
	4+300 - 6+880	Augen Gneiss	65	2.91	Locally bolts in crown 3 m long, spaced 2.5 m with occasional wire mesh, 50 mm shotcrete in crown where required.	Rockbolts of length 2.6 m long, spaced 2.2 m, 60 mm thick shotcrete

RESULTS

Parameters such as total displacement, stress distribution, and the effectiveness of installed support systems were analyzed and compared across the three geological regions. By integrating the field data, empirical classification, and finite element simulations the design assumptions and support strategies were validated. Support systems recommended by empirical relations, viz, RMR and Q-system is presented in Table 3. Detailed numerical simulation results for various tunnel chainages that includes σ_1 and σ_3, total displacements before and after support installation and support systems are presented in Table 3 for Siwaliks, Table 5 and Table 6 for Lesser Himalayas and Table 7 for Higher Himalayas respectively.

FEA Results

Finite Element Modeling included analysis of total displacement, stress distribution, and the effect of installed support systems. The numerical simulations for selected sections are shown in Fig 2 for the Siwaliks, Fig 3 for the Lesser Himalayas and Fig 4 for the Higher Himalayas. FEA shows the initial stress redistribution and deformation patterns before support installation. The results showed that total displacement varied significantly across the three geological regions. The Siwaliks region exhibited the highest displacements, which can be attributed to weak mudstone and sandstone formations, with post-support displacements exceeding 0.10 m in some sections. In contrast, lower displacement was seen in the Lesser Himalayas and Higher Himalayas, generally ranging between 0.036 m and 0.056 m, suggesting the higher strength and stiffness of quartzite and gneiss.

The displacement was correlated with the overburden and the E_m of the rock mass. Areas with lower E_m values and higher overburden demonstrated increased deformation, requiring stronger support systems. The stress concentration around the tunnel boundaries also followed predictable trends:

Maximum principal stresses (σ_1) were observed near the crowns and walls of the tunnel, particularly in zones with low RMR values. The installation of support systems significantly reduced deformation and redistributed stresses more evenly.

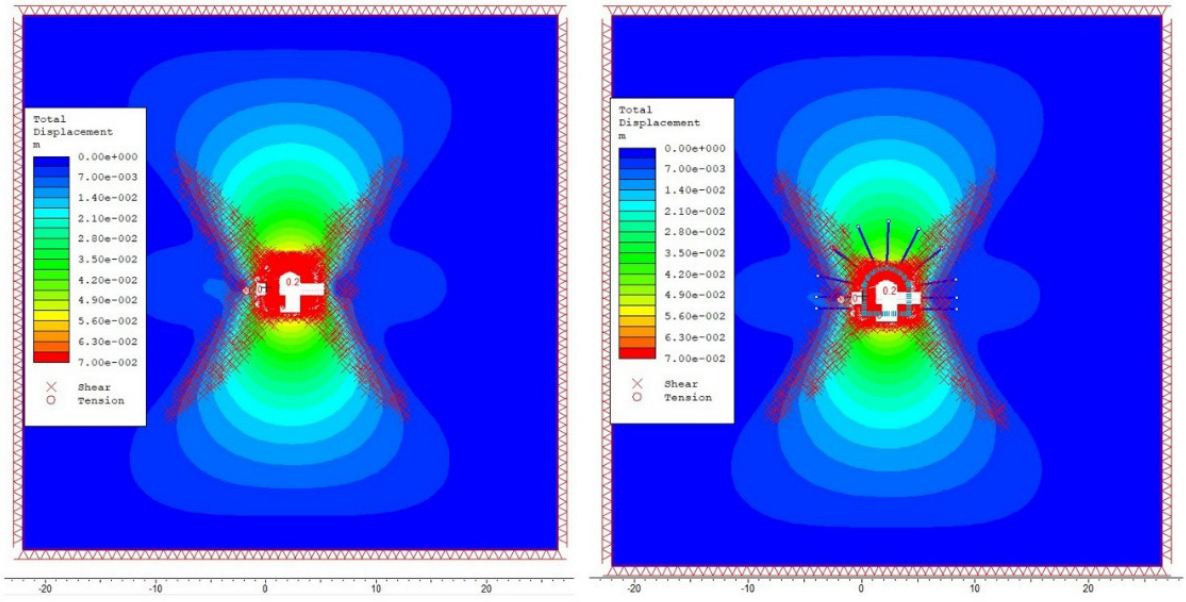

Fig. 2: Representative numerical simulation of HRT in Siwaliks before support installation and after support

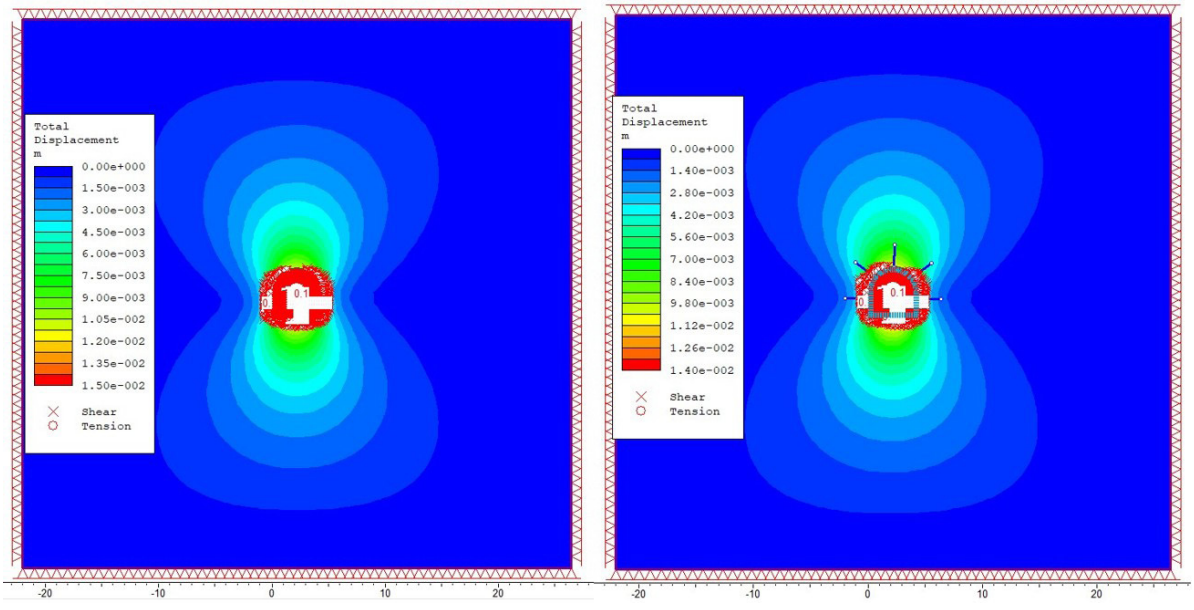

Fig. 3: Representative numerical simulation of HRT in Lesser Himalayas before support installation and after support installation

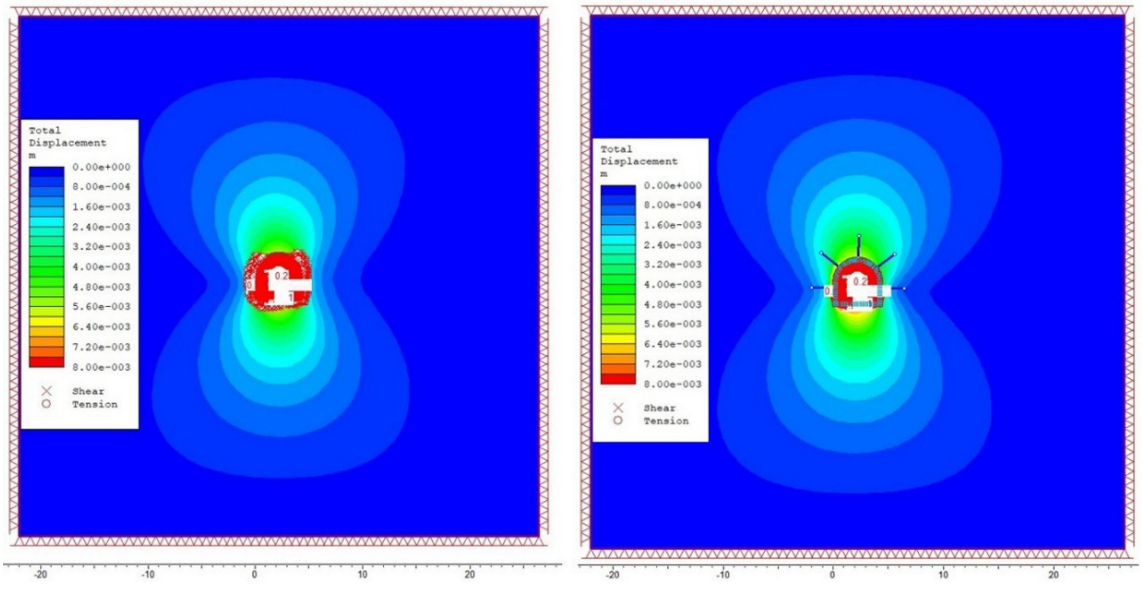

Fig. 4: Representative numerical simulation of HRT in Higher Himalayas before support installation and after support installation

Table 4: In-situ parameters for different chainages of Siwaliks

S.N.	Parameters	0+000 to 0+600	0+600 to 1+700	1+700 to 5+600	5+600 to 6+888
1	Rock Type	Sandstone	Sandstone	Mudstone	Sandstone
2	σ_1 (MPa) (Before Support)	9.81	10.22	15.82	5.27
3	σ_1 (MPa) (After Support)	12.62	13.20	18.72	6.15
4	σ_3 (MPa) (Before Support)	2.75	3.08	4.65	1.46
5	σ_3 (MPa) (After Support)	4.39	4.35	5.90	2.05
6	Total Displacement (m) (Before Support)	0.0646	0.0643	0.0820	0.0370
7	Total Displacement (m) (After Support)	0.0605	0.0606	0.0605	0.0325
8	Support Systems	FRS of thickness 8 mm at walls and crown with I beam W 360×196 at 2.5 m interval. Rockbolt of length 3.5 m at 1 m interval.	FRS of thickness 10 mm at walls and crown with I beam W 360×592 at 2 m interval. Rockbolt of length 3.5 m at 1 m interval.	FRS of thickness 10 mm at walls and crown with I beam W 360*1086 at 2 m interval. Rockbolt of length 3.5 m at 1 m interval.	FRS of thickness 8 mm at walls and crown with I beam W 360×196 at 2.5 m interval. Rockbolt of length 3.5 m at 1 m interval.

Table 5: In-situ parameters for different chainages of Lesser Himalayas

S.N.	Parameters	0+000 to 0+550	0+550 to 1+500	1+500 to 3+250	3+250 to 4+000
1	Rock Type	Quartzite	Quartzite	Sandstone	Sandstone
2	σ_1 (MPa) (Before Support)	17.42	18.05	61.90	19.34
3	σ_1 (MPa) (After Support)	15.30	19.77	54.90	20.51
4	σ_3 (MPa) (Before Support)	2.67	4.48	22.59	4.01
5	σ_3 (MPa) (After Support)	2.90	5.76	21.31	8.27
6	Total Displacement (m) (Before Support)	0.0140	0.0171	0.0118	0.0165
7	Total Displacement (m) (After Support)	0.0127	0.0155	0.0111	0.0155
8	Support Systems	FRS of thickness 5 mm at walls and crown.	FRS of thickness 5 mm at walls and crown with I beam W 360×634 at 3 m interval. Rockbolt of length 2.5 m at 2.5 m interval.	FRS of thickness 10 mm at walls and crown with I beam W 360×634 at 2 m interval. Rockbolt of length 2.5 m at 2.5 m interval.	FRS of thickness 8 mm at walls and crown with I beam W 360×463 at 3 m interval. Rockbolt of length 2.5 m at 2.5 m interval.

Table 6: In-situ parameters for different chainages of Lesser Himalayas

S.N.	Parameters	4+000 to 4+900	4+900 to 6+000	6+000 to 7+690
1	Rock Type	Sandstone	Sandstone	Sandstone
2	σ_1 (MPa) (Before Support)	15.50	20.44	11.61
3	σ_1 (MPa) (After Support)	15.64	25.12	13.22
4	σ_3 (MPa) (Before Support Installation)	3.05	5.68	2.59
5	σ_3 (MPa) (After Support)	3.80	7.77	4.62

6	Total Displacement (m) (Before Support)	0.0216	0.0146	0.0391
7	Total Displacement (m) (After Support)	0.0207	0.0121	0.0376
8	Support Systems	FRS of thickness 5 mm at walls and crown with I beam W 360*463 at 4 m interval. Rockbolt of length 2.5 m at 2.5 m interval.	FRS of thickness 10 mm at walls and crown with I beam W 360*463 at 3 m interval. Rockbolt of length 2.5 m at 2.5 m interval.	FRS of thickness 5 mm at walls and crown. Rockbolt of length 2.5 m at 2.5 m interval.

Table 7: In-situ parameters for different chainages of Higher Himalayas

S.N.	Parameters	0+000 to 1+150	1+150 to 3+300	3+300 to 4+300	4+300 to 6+880
1	Rock Type	Augen Gneiss	Augen Gneiss	Augen Gneiss	Augen Gneiss
2	σ_1 (MPa) (Before Support)	14.49	20.32	16.01	31.14
3	σ_1 (MPa) (After Support)	21.01	20.92	15.43	30.60
4	σ_3 (MPa) (Before Support)	3.32	3.90	1.92	13.54
5	σ_3 (MPa) (After Support)	4.14	4.34	2.09	14.28
6	Total Displacement (m) (Before Support)	0.00760	0.00595	0.00719	0.00382
7	Total Displacement (m) (After Support)	0.0094	0.0062	0.0059	0.0038
8	Support Systems	FRS of thickness 9 mm at walls and crown. Rockbolt of length 2.5 m at 2.5 m interval.	FRS of thickness 5 mm at walls and crown. Rockbolt of length 2.5 m at 2.5 m interval.	FRS of thickness 5 mm at walls and crown. Rockbolt of length 2.5 m at 2.5 m interval.	FRS of thickness 5 mm at walls and crown. Rockbolt of length 2.5 m at 2.5 m interval.

SUPPORT SYSTEM OPTIMIZATION

Support systems were initially proposed based on empirical RMR recommendations. It included a combination of FRS, rock bolts, and in some cases, steel sets. The initial support design was later validated and optimized by numerical modeling to make sure FoS was more than 1.5 in all sections. In Siwaliks, where displacement was largest, a thicker FRS (40 mm) and longer bolts (up to 4 m) were required. Compared to that, the Lesser Himalayas and Higher Himalayas required thin shotcrete layers (25–30 mm) and short bolts (2.5–3 m) because the quality of the rock mass was higher. The modeling results confirmed that after support installation, displacements were reduced by 20–40%, and stress concentrations were mitigated. This showed the effectiveness of the support systems used and allowed for optimization to avoid over-design while maintaining stability. The final installed support system for each tunnel segment was selected to balance between safety and cost effectiveness, suitable for the geological conditions of the area.

Stress Redistribution Relative to Overburden

There is redistribution of stress before the support installation due to release of confining pressure, leading to stress concentration at undesirable points along the tunnel path. The HRT of Higher Himalayas produced the highest average stress-to-overburden ratio, followed by the HRT of Lesser Himalayas, whereas the HRT of the Siwaliks produced the lowest stress levels. This is because of the solid geological condition in the Higher Himalayan Region.

It is also noted that the tunnel in the Lesser Himalayas develops the highest average stress. This can be attributed to the fact that the project area in the Lesser Himalayas has the highest overburden values compared to the other regions (ranging up to 770 m). This shows that the overburden pressure also plays a significant role in stress generation.

Subsequent to installation of the support system, the ratio of stress to overburden is increased slightly, mostly due to the load-sharing phenomenon of the installed support systems. The support systems do not, however, decrease the maximum principal stress significantly, but stabilize the tunnel by redistributing loads and avoiding excessive deformations. The stress ratio variation in the three regions follows the lithological and rock mass differences, strengthening the argument for site-specific reinforcement measures.

In the case of the Lesser Himalayas, the stress-to overburden ratio remained nearly constant before and after support installation. This can be attributed to the moderately stiff and relatively homogeneous rock mass which predominantly consists of quartzite and compact sandstone combined with high overburden, which provides substantial confinement. As a result, the HRT in this region maintained a relatively stable stress regime even during excavation, and the role of support was primarily preventive. Unlike in the Siwaliks or the Higher Himalayas, where stress redistribution is more noticeable, the stable geology and confinement resulted in limited variation in stress ratio post-support. A comparative graph of showing ratio of average stress (σ_1) to overburden before and after support installation is shown in Fig 5.

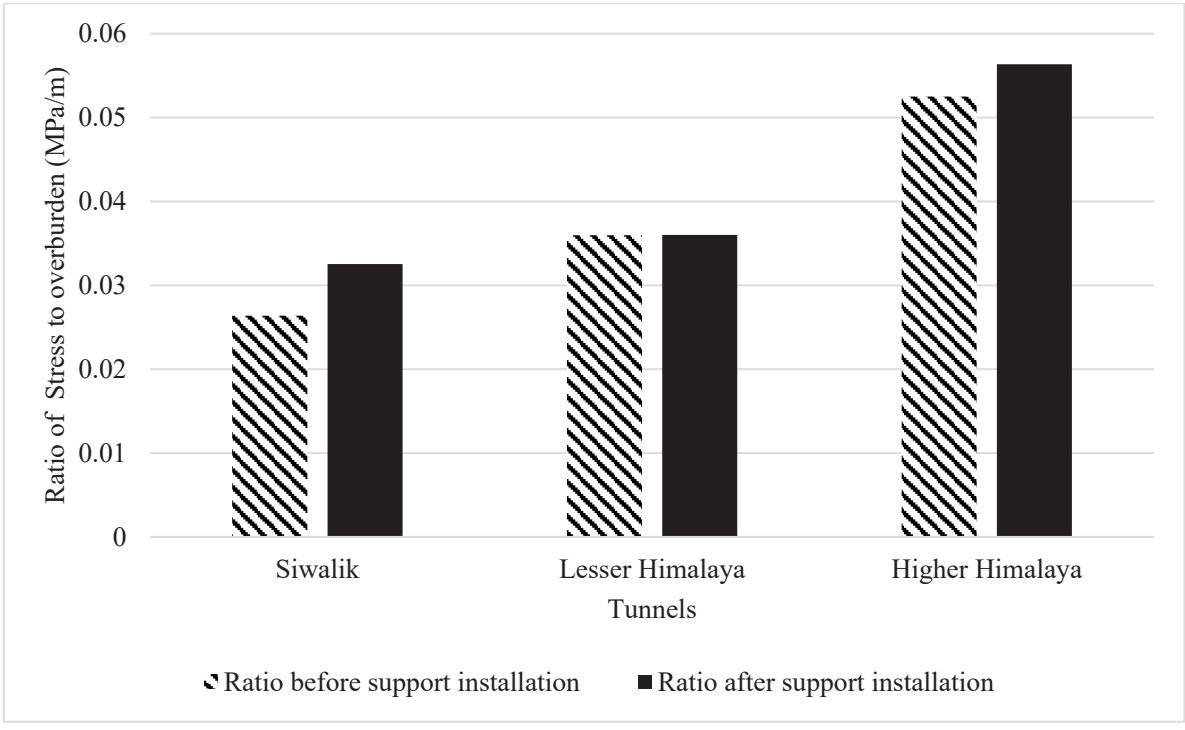

Fig. 5: Bar chart showing ratio of average stress (σ_1) to overburden before and after support installation

DISPLACEMENT-TO-DEFORMATION MODULUS RATIO ANALYSIS

The average displacement shows the deformation behavior of the rock mass under varying stress conditions. The ratio of average total displacement to deformation modulus provides a measure of the relative deformability of the rock mass before and after the installation of support. A higher ratio indicates a more deformable rock mass, whereas a lower ratio suggests greater stiffness and resistance to movement.

Before the installation of support, the displacement-to deformation modulus ratio is highest in the Siwaliks region, followed by the Lesser Himalayas and the Higher Himalayas. This corresponds to the geological properties of these regions, with the Siwaliks being composed of weaker, highly fractured rock masses, having low modulus of deformation resulting in greater displacements for the same applied stresses.

After the installation of support, the displacement-to deformation modulus ratio is reduced across all regions, demonstrating the effectiveness of reinforcement in limiting tunnel deformations. The reduction is most significant in the HRT of Siwaliks region, where intensive support systems (e.g., thicker fiber-reinforced shotcrete and closer steel sets and rock bolt spacing) were required to enhance tunnel stability.

Conversely, the HRT of Higher Himalayas showed minimal reduction in deformation, as the rock mass shows high stiffness and lower deformation tendencies. The ratio of average total displacement to deformation modulus before and after support installation showed little to no change. This further indicates that despite experiencing high stress levels, the strong and stiff rock mass in this region, enhanced by effective early confinement, limited the deformation. In this case, the support system primarily served to ensure long term stability, rather

than significantly altering the mechanical response, which was already inherently strong due to favorable lithological conditions. A bar chart showing ratio of average total displacement to deformation modulus before and after support installation is shown in Fig 6.

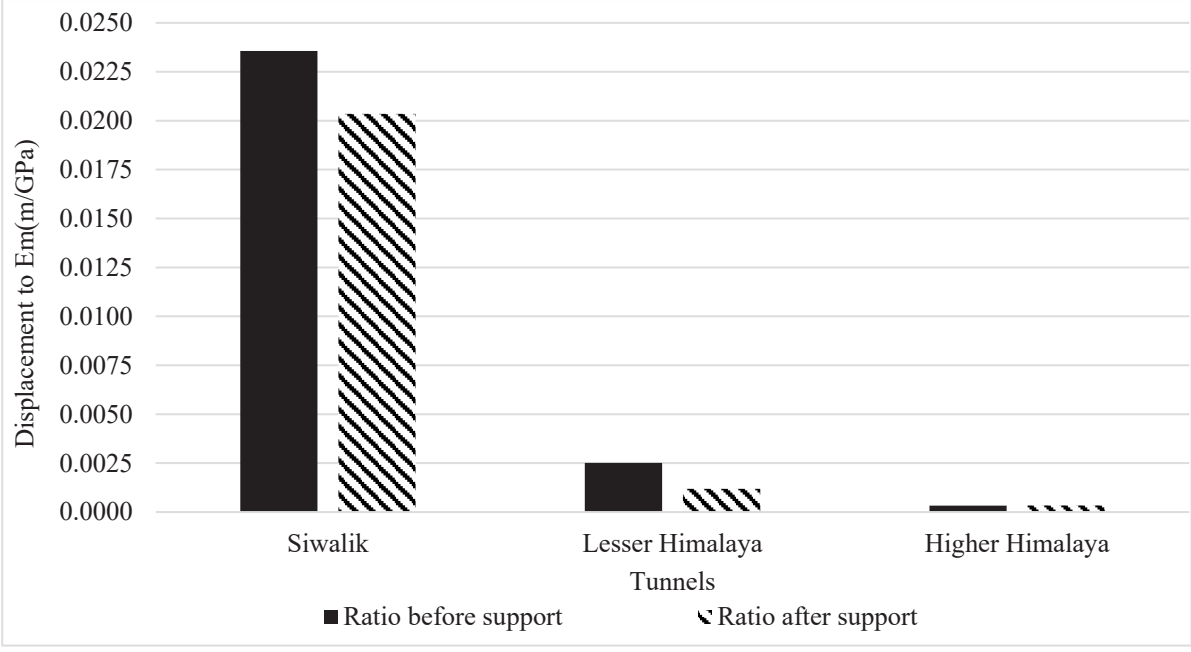

Fig. 6: Bar chart showing ratio of average total displacement to deformation modulus before & after support installation

Stress (σ_1) Before Support Installation Along the Tunnel

The stress distribution along the tunnel chainage before the application of support systems shows the stress concentration at various points along the tunnel alignment. The stress distribution trend for Siwaliks, Lesser Himalayas, and Higher Himalayas follows a varying pattern, with some sections experiencing significantly higher stress than others.

These variations can be due to changes in rock mass properties, lithological variations, overburden, and geological structures along the tunnel alignment. In sections where stress concentrations are high, additional reinforcement measures such as systematic bolting, reinforced shotcrete, or steel sets may be required to prevent excessive deformation and potential failure. A graph showing stress before installation of support along the tunnel alignment is shown in Fig 7.

Total Displacement Before Support Installation Along the Tunnel

The displacement profile along the tunnel chainage shows how the deformation behavior changes along different sections of the tunnel. Similar to the stress distribution, displacement varies with chainage, with some sections experiencing more movement due to weaker rock formations or increased overburden pressures. A graph showing the total displacement before installation of support along the tunnel alignments is shown in Fig 8.

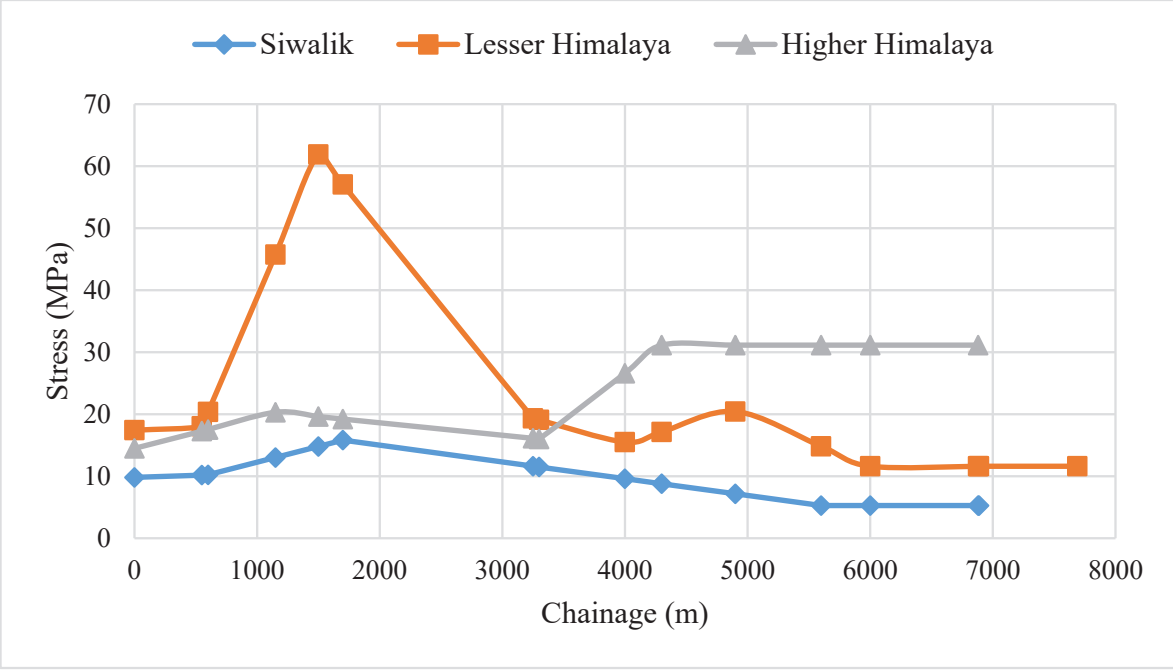

Fig. 7: Graph showing stress before support installation along the tnnel alignment

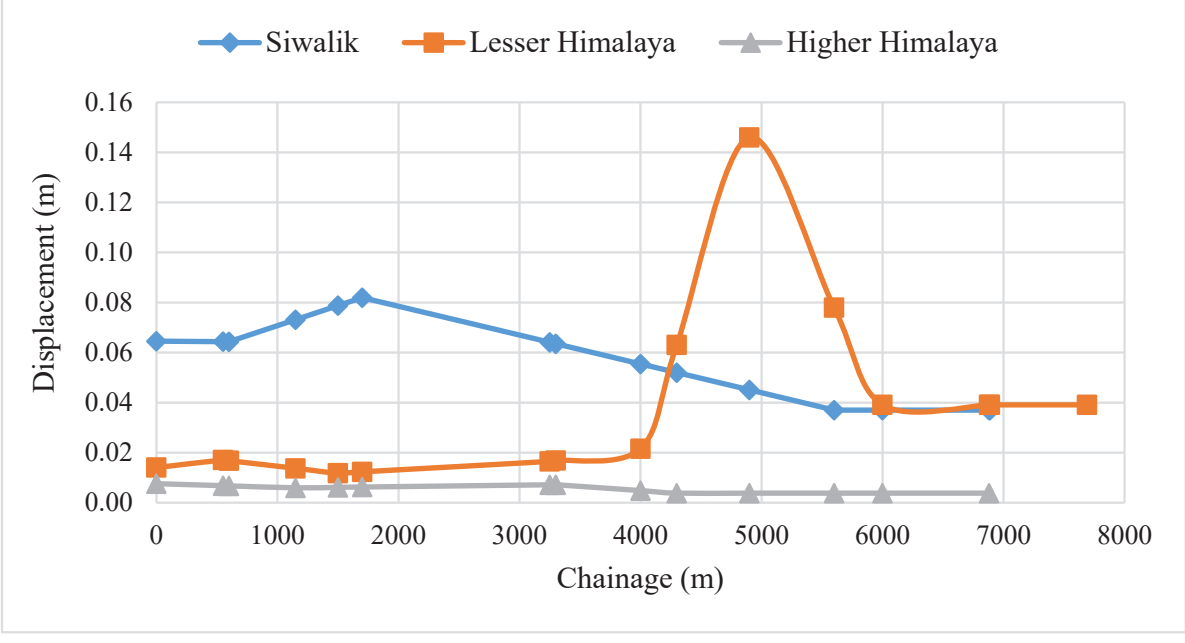

Fig. 8: Graph showing total displacement before support installation along the tunnel alignment

DISCUSSIONS

The comparative evaluation reveals clear lithological and mechanical contrasts between the three regions. The deformability and stiffness analysis reveals Siwaliks are highly deformable due to low deformation modulus and weak rock fabric. Higher Himalayas show stiffness from metamorphic rock masses. High overburden in Lesser Himalaya and Higher Himalaya significantly affects major principal stress values despite decent rock quality, emphasizing the compounded role of lithology and depth. The Siwaliks region consists of generally lower over- burden compared to the Lesser Himalayas and Higher Himalayas. In Siwaliks, intensive support like thicker FRS, closer I-beams and bolts was necessary. In contrast, Lesser and Higher Himalayas required simpler, cost-effective systems due to inherent geological stability Redistribution of stress patterns correlated well with RMR and GSI values, confirming the predictive power of empirical classification systems.

Although hydrogeological modeling was not directly included in this study, the engineering geological reports indicate variable groundwater conditions. The Siwaliks region, which has young sedimentary rocks such as mudstone and sandstone, is prone to higher groundwater inflows due to its porous and fractured nature. This may result in greater deformation and require strong drainage and support measures. In contrast, the Lesser Himalayas and Higher Himalayas, which have more compact quartzite and gneiss formations, showed relatively limited groundwater access and more stable drainage conditions. These differences in drainage and groundwater behavior partially explain the higher support requirements observed in the Siwaliks and should be considered during construction planning and long-term maintenance.

LIMITATIONS

This study presents certain limitations that highlight directions for future studies:

1. The analysis relies solely on empirical and numerical methods without validation from in-situ instrumentation or monitoring during construction. Integrating field monitoring data would help validate the models.
2. Two-dimensional numerical modelling was employed in this study, which may not fully capture the real word complexities. Performing three-dimensional numerical modelling can provide more accurate and comprehensive simulation results.

CONCLUSION

This study highlights the critical role of geological setting in tunnel deformation behavior and support requirements. Based on numerical and empirical analyses of three contrasting Himalayan regions.

1. Displacements in the Lesser and Higher Himalayas were 38.64% and 90.09% lower than in the Siwaliks, respectively.
2. The ratio of major stress to overburden was 36.33% higher in the Lesser Himalayas and 98.98% higher in the Higher Himalayas compared to the Siwaliks.
3. The Higher Himalayas showed the highest deformation modulus, indicating stiffer, more stable rock, whereas the Siwaliks had more fractured, deformable formations.

Consequently, the tunnels in the Siwaliks require the strong support systems to ensure stability, including thicker shotcrete layers, closer spacing of steel sets, and longer rock bolts. The Lesser Himalayas displayed moderate mechanical behavior, necessitating balanced and site-specific support designs influenced by both lithology and high overburden. In contrast, the Higher Himalayas presented the most favorable conditions for tunneling, with minimal deformation and reduced support demands despite undergoing higher stress levels, owing to competent rock formations.

Support systems significantly improve tunnel performance but cannot substitute for poor geological conditions. Hence, geology specific tunnel support strategies must be adopted rather than relying on uniform design standards.

While the reliance on secondary data is a limitation, it allows a realistic and resource-efficient approach in early project phases. Future studies should integrate in-situ monitoring and 3D modeling to validate and refine these findings.

This study showed that geological conditions have a significant influence on the deformation and support behavior of HRTs. The results highlight the necessity of geology- specific tunnel support strategies, as rock mass properties and overburden stress play a more critical role to tunnel performance and stability than the support systems.

ACKNOWLEDGEMENT

The authors are very grateful to Sujan Maka and Subeg Man Bijukchhen from Khwopa Engineering College, Prayag Maharjan from Hydro-Consult Engineering Ltd. and Bibek Thapa and Raju Miyan from Khwopa College of Engineering for their valuable insights and suggestions during various phases of the study. We would also like to express our sincere gratitude Khwopa College of Engineering for providing the platform to carry out this study successfully.

AUTHOR CONTRIBUTIONS

The study was conceptualized by Nirmal Kafle and Aanand Kumar Mishra, both of whom also provided overall academic supervision. Aashika Koju carried out the literature review, rock mass classification and analysis of stress-displacement behavior. Balkrishna Jha was responsible for the final result analysis, discussion, visualization including charts and figures and preparation of comparative tables. Ijan Shrestha did the analysis part and drafted the reports. All the authors contributed equally to the project and reviewed and approved the final version of the manuscript.

CONFLICT OF INTEREST

The authors declare that the paper has not previously published in another journal/bulletin.

REFERENCES

Abbas, N., Li, K., Fissha, Y., Lei, W., Emad, M. Z., Chandrahas, N. S., Pradhan, B., Chelani, A., Aydin, A. and Cheepurupalli, N. R., 2024. Stress-deformation and stability challenges in Himalayan tunnels: impact of geological discontinuities. Discover Materials, 4(1). https://doi.org/10.1007/s43939-024-00144-z.

Aydan, Ö., 2019. Rock Mechanics and Rock Engineering. London: CRC Press.https://doi.org/10.1201/9780367822293.

Azad, M. A., Naithani, A. K., Shekhar, S., Ahmad, S. and Singh, S. K., 2023. Tunnel Support Validation Using Numerical Modelling: A Case Study from NW HImalaya. Indian Geotechnical Journal, 4335-4349. doi:10.1007/s10706-023-02506-5.

Bieniawski, Z., 1978. Determining Rock Mass Deformability: Experience from Case Histories. International Journal of Rock Mechanics and Mining Sciences, 237-247. https://doi.org/10.1016/0148-9062(78)90956-7.

Bieniawski, Z., 1989. Engineering Rock Mass Classifications: A Complete Manual for Engineers and Geologists in Mining, Civil and Petroleum .

Dhital, M. R., 2015. Geology of the Nepal Himalaya: Regional Perspective of the Classic Collided Orogen. Berlin: Springer.DOI 10.1007/978-3-319-02496-7.

Hoek, E. and Brown, E.T., 2018. The Hoek–Brown failure criterion and GSI – 2018 edition. Journal of Rock Mechanics and Geotechnical Engineering, 445-463. https://doi.org/10.1016/j.jrmge.2018.08.001.

Grimstad, E. and Barton, N., 1993. Updating the Q-system for NMT. Proceedings of the International Symposium on Sprayed Concrete, (pp. 46-66).

Hoek, E. and Diederichs, M.S., 2006. Empirical Estimation of Rock Mass Modulus. International Journal of Rock Mechanics and Mining Sciences. , 43(2), 203-215. https://doi.org/10.1016/j.ijrmms.2005.06.005.

Li, C. C., 2017. Principles of rockbolting design. Journal of Rock Mechanics and Geotechnical Engineering, 396--414. https://doi.org/10.1016/j.jrmge.2017.04.002.

Palmström A. and Stille H., 2014. Rock Engineering. Emerald Publishing Limited.

Panthi, K. K., 2004. Tunnelling challenges in Nepal. BERGMEKANIKK/GEOTEKNIKK. 2004.

Panthi, K. K., 2008. Underground Space for Infrastructure Development and Engineering Geological Challenges in Tunneling in the Himalayas. Hydro Nepal: Journal of Water, Energy and Environment, 1, 43-49. https://doi.org/10.3126/hn.v1i0.890.

Paudyal H. and Panthi A., 2010. Seismic vulnerability in the Himalayan region. Himalayan Physics, 14-17. https://doi.org/10.3126/hj.v1i0.5165.

Serafim, J.L. and Pereira, J.P., 1983. Considerations on the Geomechanical Classification of Bieniawski. Proceedings of International Symposium on Engineering Geology and Underground Openings , (pp. 1133-1144).

Shah S.P., and Rangan B.V., 1971. Fiber reinforced concrete properties.

Sheorey, P., 1994. A theory for In Situ stresses in isotropic and transverseley isotropic rock. International Journal of Rock Mechanics and Mining Sciences, 23-34.

Thapaliya, B., Shrestha, N., Acharya, M. S., Yadav, S. K. and Thapa, P. B., 2025. Computational optimization of tunnel support systems under static and dynamic loads in the Himalayan region. Geotechnical and Geological Engineering, 43(6), 302.https://ui.adsabs.harvard.edu/link_gateway/2025GGEng..43..302T/doi:10.1007/s10706-025-03273-1.

Upreti, B., 1999. An overview of the stratigraphy and tectonics of the Nepal Himalaya. Journal of Asian Earth Sciences, 577--606.

Upreti, B., 2001. The Physiography and Geological Division of Nepal and Their Bearing on the Landlside Problem.

Yin A. and Harrison T. M., 2000. Geologic evolution of the Himalayan-Tibetan orogen. Annual Review of Earth and Planetary Sciences, 211--280.